Science and Innovation of Advanced Materials

The Materials Research Society of Thailand

Research Article

Green Selective Oxidized Microcrystalline Cellulose and Its Use in Encapsulation of Lavender Essential Oils

Gone Yi Thaw Maung[1], Chariya Kaewsaneha[1], Atitsa Petchsuk[2], Pakorn Opaprakasit[1,*]

[1]Integrated Science and Innovation, Sirindhorn Institute of Technology (SIIT), Thammasat University, Pathum Thani 12120, Thailand
[2]National Metal and Materials Technology Center (MTEC), National Science and Technology Development Agency (NSTDA), Pathum Thani 12120, Thailand

* Corresponding author e-mail: pakorn@siit.tu.ac.th

Received: *November 28th, 2024* | ***Revised:*** *June 15th, 2025* | ***Accepted:*** *June 15th, 2025*

DOI: 10.48048/siam.2025.68008

Abstract: Microcrystalline cellulose (MCC) has emerged as a promising bio-based material due to its abundance, degradability, and biocompatibility. This study focuses on the chemical modification of MCC to enhance its amphiphilicity and use to encapsulate lavender essential oil (LO) for cosmetic applications. MCC was selectively oxidized by a green process using 2,2,6,6-tetramethyl-1-piperidinyloxy (TEMPO) and ozone co-oxidants. The reaction mechanisms and the chemical structures of the oxidized MCC products were examined by iodometric titration, UV-Vis, and FTIR spectroscopy. The degree of oxidation (DO), i.e., the conversion of -OH to -COOH/-COO- groups, is dependent on the reaction time and acid concentration, in which a suitable sample with optimum carboxylate content was obtained using 0.1 M H_2SO_4 and 2-hour ozonation time. The resulting amphiphilic MCC was employed to encapsulate LO in an ethanol/water medium. The effect of the ethanol/water ratio on the stability and encapsulation efficiency of LO-loaded MCC (LO@MCC) was studied. Zeta potential measurement, SEM, and FTIR spectroscopy were used to confirm the encapsulation and morphology of the materials. An appropriate ethanol/water ratio (60/40) led to a high encapsulation efficiency (EE%) and high loading capacity (LC%) of 79.1 and 30.8 %. The results confirm that in the oxidation process, MCC molecules were oxidized, converting hydroxyl groups to carboxylates. Chain scission also occurred, leading to soluble small-sized MCC, while most remained insoluble fragments with high surface charges, forming stable dispersing particles. In the LO encapsulation process, the soluble MCC acts as a surfactant and shell structure, forming LO-encapsulated droplets deposited on the dispersing MCC particles. The materials have a high potential for use in cosmetic applications.

Keywords: Microcrystalline cellulose, Encapsulation, Lavender oil, TEMPO, Selective oxidation

1. Introduction

Nowadays, environmental issues resulting from the use of petroleum-derived polymers have led to significant growth in the demand for eco-friendly materials in the packaging, coating, cosmetics, and agriculture sectors [1]. Developing sustainable and green modification processes for natural polymers has gained significant attention in response to these demands. Among these, green oxidation methods for polysaccharides, such as cellulose, offer environmentally friendly alternatives to conventional chemical modifications by reducing hazardous waste, energy

* The work was presented at The 22nd International Symposium on Eco-materials Processing and Design (ISEPD2024) 21 - 24 January 2024

consumption, and toxic reagents [2]. These eco-conscious strategies align with global sustainability goals and enhance the functional properties of biopolymers for advanced material applications. Cellulose, the most abundant natural biopolymer, has drawn attraction owing to its renewability, recyclability, sizable surface area, lightweight, and affordable pricing. MCC is a derivative of cellulose that is mostly produced from wood fibers by acid hydrolysis [3,4]. It is an anionic biopolymer with a high aspect ratio and bending strength commonly used in synthetic composites. The reinforcing phase has a high cellulose content and crystallinity [5]. Due to its high specific surface area, distinct physicochemical characteristics, and renewability, MCC has considerable potential for drug delivery, biocomposites, protein immobilization, and metallic reaction templates [6]. Beyond these applications, MCC has recently attracted interest in the cosmetic industry due to its excellent biocompatibility, stability, and ability to form stable dispersions. These properties make MCC an ideal candidate for use as a rheology modifier, stabilizer, and carrier in various skincare and personal care formulations. Its natural origin and biodegradability further contribute to the development of sustainable cosmetic products, aligning with the industry's shift towards eco-friendly and safe ingredients [7].

Lavender oil (LO) is a frequently used essential oil in biomedical applications because of its antibacterial, antifungal, antioxidant, and muscle relaxant qualities. However, LO is highly volatile and becomes unstable when exposed to air, light, heat, or moisture. Consequently, an approach that increases LO stability, provides a controlled release and lengthens the action period is needed [8]. Encapsulation has been widely employed to improve essential oils' stability, bioavailability, and controlled release in various applications, including food, pharmaceuticals, and cosmetics. Recent studies have demonstrated that encapsulation techniques, particularly using passive adsorption and polymer-based carriers, effectively protect essential oils from degradation caused by oxidation, heat, and moisture, thereby enhancing their functional properties [9,10].

This work aims to develop oxidized MMC using an environmentally friendly method employing 2,2,6,6-tetramethyl-1-piperidinyloxy (TEMPO). The effect of oxidization conditions on the degree of oxidation, chemical structures, and properties of the oxidized MCC is investigated. The materials are used to encapsulate LO, employing an easy passive loading method. The influence of EtOH/water mixture ratios on the stability and encapsulation effectiveness of the produced LO@MCC particles is examined. The materials have a high potential for use in cosmetic applications.

2. Methodology

2.1 Materials

MCC (laboratory-grade) and TEMPO (≥98% purity) were purchased from U&V Holding Company. LO was obtained from Krungthep Chemi. Dimethyl sulfoxide (DMSO) (≥99.9% purity), sulfuric acid (H_2SO_4) (95–98% purity), and sodium hydroxide (NaOH) (≥98% purity) were supplied by Carlo Erba Chemicals. All chemicals were used without further purification.

2.2 Preparation of oxidized MCC and LO-encapsulated MCC

The oxidized MMC was synthesized using an environmentally friendly method employing TEMPO. Initially, $TEMPO^+$ was prepared by ozone oxidation of TEMPO under optimized conditions by feeding ozone for 2 h. A solution of TEMPO (0.512 mmol) in 10 mL of water was stirred until no TEMPO solid was observed at 4-5°C, followed by adding 10 mL of H_2SO_4 acid at various concentrations from 0.05 M to 0.10 M. The effect of acid concentration on converting TEMPO to $TEMPO^+$ was investigated. The concentration of the resulting $TEMPO^+$ solution was measured by UV-Vis spectroscopy and iodometric titration. The freshly prepared $TEMPO^+$ solution was then added to the MCC solution. The oxidation degree of oxidized MCC was also determined by conductivity titration, in which 0.01 M HCl and 0.125 M NaOH solutions were used as standard solutions [11].

A passive loading method was used to encapsulate LO into MCC. LO was agitated at 250 rpm for 5 min, after being dispersed in 40 mL of ethanol/water at various volume ratios, i.e., 0/100, 20/80,40/60, 50/50, 60/40, 80/20, and 100/0. Following that, LO was dissolved in ethanol solvent and then gently combined with the aqueous phase of MCC. The resulting mixture was vortexed for two min at 150 rpm. The mixture was then shaken using a Heidolph

Rotamax 120 for 24 h at 150 rpm. The unentrapped LO in the supernatant was then separated using a high-speed centrifuge (Avanti JXN-26 centrifuge) for 30 min at 25,000 rpm. Finally, LO-encapsulated MCC (LO@MCC) precipitates were acquired [12].

2.3 Characterization

A UV-Vis spectrophotometer (UV-1800, Shimadzu) was applied to determine the concentration of TEMPO and $TEMPO^+$ in the conversion process, EE%, and LC%, using quartz cuvettes with ethanol-water supernatant dispersions. The $TEMPO^+$ conversion was calculated using the absorption bands at 290 and 480 nm and the LO encapsulation at 250 nm. A microelectrophoresis device (Zetasizer; Malvern, Nano ZS) was used to characterize the prepared encapsulated samples' particle size and zeta potential. Before measurements, the samples were diluted and spread in 10 ml of deionized water. Each sample's zeta potential and particle size were measured at 25 °C in triplicate. A scanning electron microscope (SEM; JEOL, JSM7800F) was used to investigate the sample's morphology. A Fourier transform infrared (FTIR) spectrometer operating in attenuated total reflection mode (ATR-FTIR; Nicolet iS50, Thermo Scientific) was used to examine the chemical structures and functional groups of the oxidized particles with 32 scans at 4 cm^{-1} resolution.

3. Results and discussion

Effects of acid on TEMPO to $TEMPO^+$ conversion by UV-Vis spectroscopy and iodometric titration

UV-Vis spectra were used to quantitatively determine the concentrations of TEMPO and $TEMPO^+$ in the solutions. The characteristic bands of TEMPO (250 and 400 nm), $TEMPO^+$ (290 and 480 nm), and TEMPOH (200 and 315 nm) were employed [11]. Calibration curves for $TEMPO^+$ vs. acid concentrations were created using the iodometric titration results in conjunction with UV-Vis spectra, as shown in Figure 1. The graphs showed a high correlation, with R^2 of 0.994 and 0.991, respectively. The acidic environments cause TEMPO to change reversibly to $TEMPO^+$ and TEMPOH, which is then further transformed to protonated TEMPOH-H^+. This proves that $TEMPO^+$ contents increase with the increased acid concentration. The findings show that throughout the two-hour disproportionation period, the quantities of TEMPO consumption and $TEMPO^+$ production grow linearly as a function of time. Due to the production of hydroxylamine and protonated hydroxylamine, the amount of TEMPO consumed increases significantly with time relative to the amount of created $TEMPO^+$.

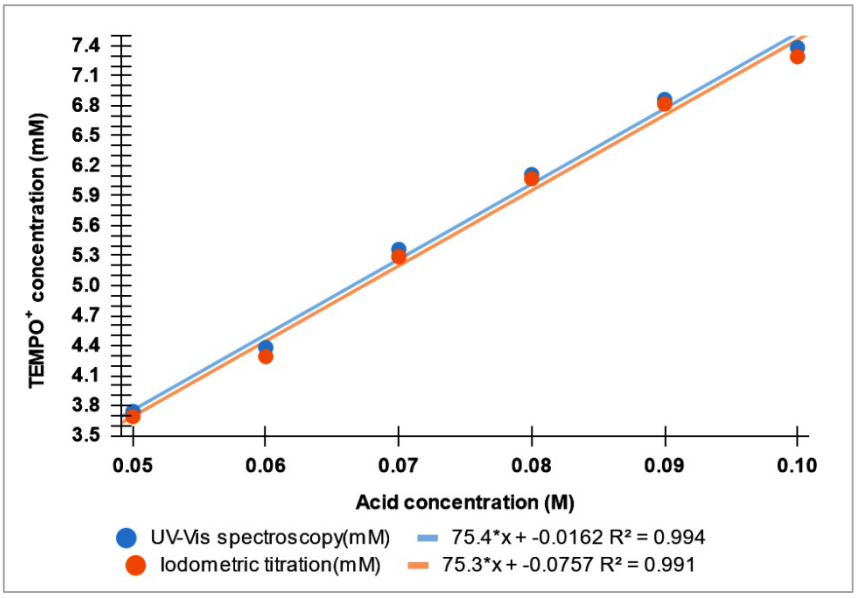

Figure 1 Standard curves illustrating the $TEMPO^+$ contents as a function of acid concentration, as determined by iodometric titration and UV-Vis spectroscopy.

The conversion of TEMPO to TEMPO$^+$ increased with the ozone dispersion time, showing a high R^2 value in a linear relationship, as summarized in Figure 2. However, the increased TEMPO$^+$ concentration has become nearly constant after 2 h. Thus, it can be concluded that a two-hour dispersal time is the optimum for converting TEMPO to TEMPO$^+$.

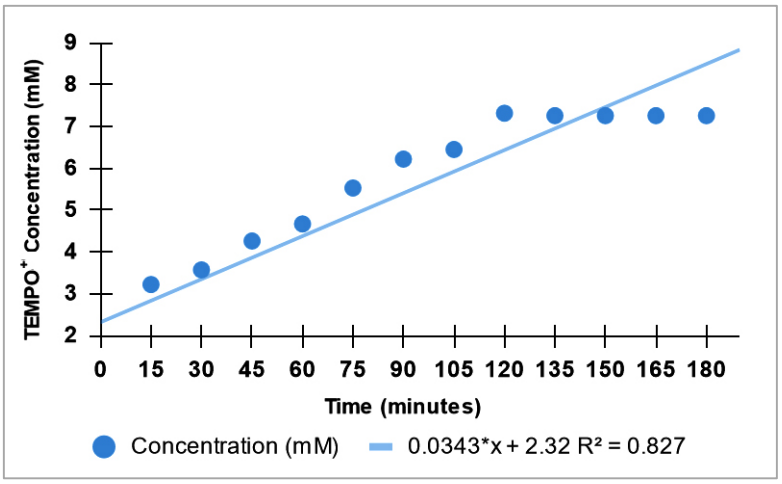

Figure 2 A standard curve illustrating the correlation between TEMPO$^+$ concentration and its dispersal time from an ozone generator.

Effect of TEMPO$^+$ concentration on oxidation degree of MCC

The generated oxoammonium (TEMPO$^+$) was used to oxidize MCC. The effect of its concentration on the degree of oxidation of MCC was investigated. FTIR spectroscopy was employed to examine the samples' functional groups and chemical structures. FTIR spectra of MCC and its corresponding oxidized MCCs are compared in Figure 3.

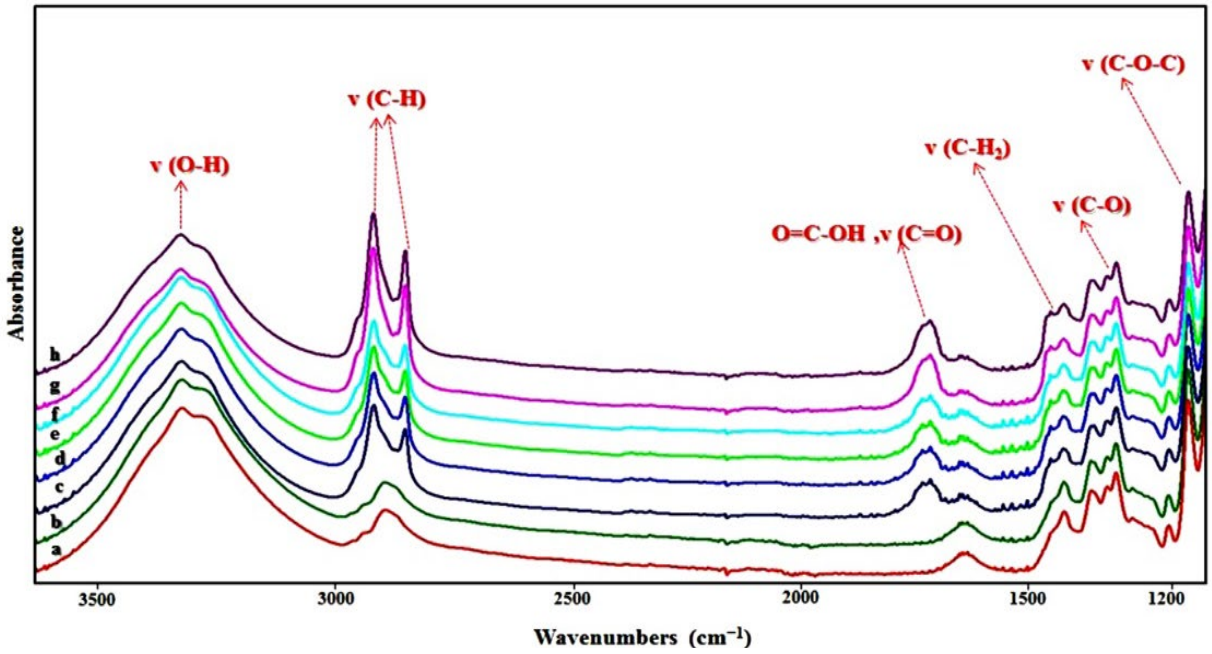

Figure 3 (a) FTIR spectra of native MCC, (b) Oxidized MCC by TEMPO in the absence of acid, and (c–h) Oxidized MCC produced at various oxoammonium concentrations: 3.741, 4.380, 5.363, 6.110, 6.862 and 7.381 mM/g of MCC.

Native MCC showed a broad band at 3550-3200 cm^{-1}, associated with the O-H stretching of hydroxyl groups. The C-H stretching modes at 2980-2850 cm^{-1} are masked by their highly crystalline nature as a broad single band. The C-O and C-O-C bands are observed at 1350-1300 and 1175 cm^{-1}, respectively. The FTIR spectrum of oxidized MCC in the absence of acid shows significantly similar patterns to native MCC, reflecting a slight degree of oxidation. In contrast, drastic changes are observed in MCC samples after being oxidized in the presence of acids, i.e., with oxoammonium, at different concentrations. The sharp C=O stretching band at 1716-1734 cm^{-1} indicated a formation of carboxylic acid due to the oxidation of its hydroxyls by $TEMPO^+$. Conductivity titration was also used to calculate the degree of oxidation (DO) of MCC, as summarized in Table 1.

The C-H stretching bands of the oxidized MCC at 2980-2850 cm^{-1} are separated, as the oxidation also led to a lower degree of crystallinity. An appearance of 1716-1734 cm^{-1} bands indicated that an increase in the oxoammonium content caused an elevation in the carboxylic acid contents, also known as the oxidation degree (OD), in the structure of MCC. The oxidation reaction produced a large number of free carboxylic acid groups on the molecular structure and a high carboxylate in C-6 at a $TEMPO^+$ level of 7.37 mM, which was oxidized by 0.1 M H_2SO_4.

Table 1 The oxidation degree (OD) of oxidized MCC by conductivity titration

MCC treated by	Concentration of NaOH (M)	Dry weight of sample (g)	Volume of NaOH at 2nd and 3rd phase (mL)	Total COO^- contents (μmol/g)
TEMPO+0.1M H_2SO_4	0.125	0.04	15.5	48.4
TEMPO+0.09M H_2SO_4	0.125	0.04	14.6	45.6
TEMPO+0.08M H_2SO_4	0.125	0.04	14.2	44.4
TEMPO+0.07M H_2SO_4	0.125	0.04	13.8	43.1
TEMPO+0.06M H_2SO_4	0.125	0.04	13.5	42.2
TEMPO+0.05M H_2SO_4	0.125	0.04	13	40.6

Encapsulation of LO and immobilization on oxidized MMC

The oxidized MCC was employed to encapsulate LO for cosmetic applications. As oxidized MCC can partially dissolve and disperse in water, while LO is dissoluble in ethanol, an EtOH/water mixture at different ratios was employed in the encapsulation process. The zeta potential, particle size, EE%, and LC% were examined as a function of EtOH/water ratios, as summarized in Table 2 and Figure 4. The results of EE% (68.5 to 79.1) and LC% (26.7 to 30.8) of the samples prepared at different EtOH/water ratios showed slightly different values, indicating a slight effect on the mixing ratio. A 60:40 ratio showed the highest values at 79.1% and 30.8%, respectively. This ratio balances the solubility of LO, which is more soluble in ethanol than water, facilitating better dispersion within the emulsion. MCC particles can effectively stabilize the oil-water interface at this solvent ratio, forming a robust Pickering emulsion. This likely results in favorable emulsion properties, such as appropriate droplet size and stability, contributing to higher encapsulation efficiency and loading capacity. The zeta potential of neat oxidized MCC ranges from -20 to -23 mV, indicating deprotonated surface carboxyl groups. After LO encapsulation, the zeta potential changes from -27 to -33 mV, suggesting increased negative charge deposition on MCC. The value insignificantly varies with the EtOH/water ratio. The corresponding LO-encapsulated samples showed higher negative zeta potential values at -27 to -33 mV. The value increased with the content of EtOH in the medium, indicating the deposition of more negative charges on the MCC particle's surfaces. The higher negative value leads to higher particle dispersing stability, preventing agglomeration of the particles. This is reflected by the smaller average size of the LO-encapsulated samples compared to neat dispersing MCC. The smallest average sizes of the samples prepared using a medium at a 60:40 ratio also confirm the stabilization efficiency.

Table 2 Encapsulation efficiency (EE%) and loading content (LC%) of LO on oxidized MCC using EtOH/water medium at different ratios

Samples	Ratio of EtOH/water	Encapsulation efficiency (%)	Loading capacity (%)
LO@MCC 1	0:100	68.5	26.7
LO@MCC 2	20:80	68.7	26.8
LO@MCC 3	40:60	69.9	27.3
LO@MCC 4	50:50	74.5	29.0
LO@MCC 5	60:40	79.1	30.8
LO@MCC 6	80:20	73.2	28.5
LO@MCC 7	100:0	71.2	27.8

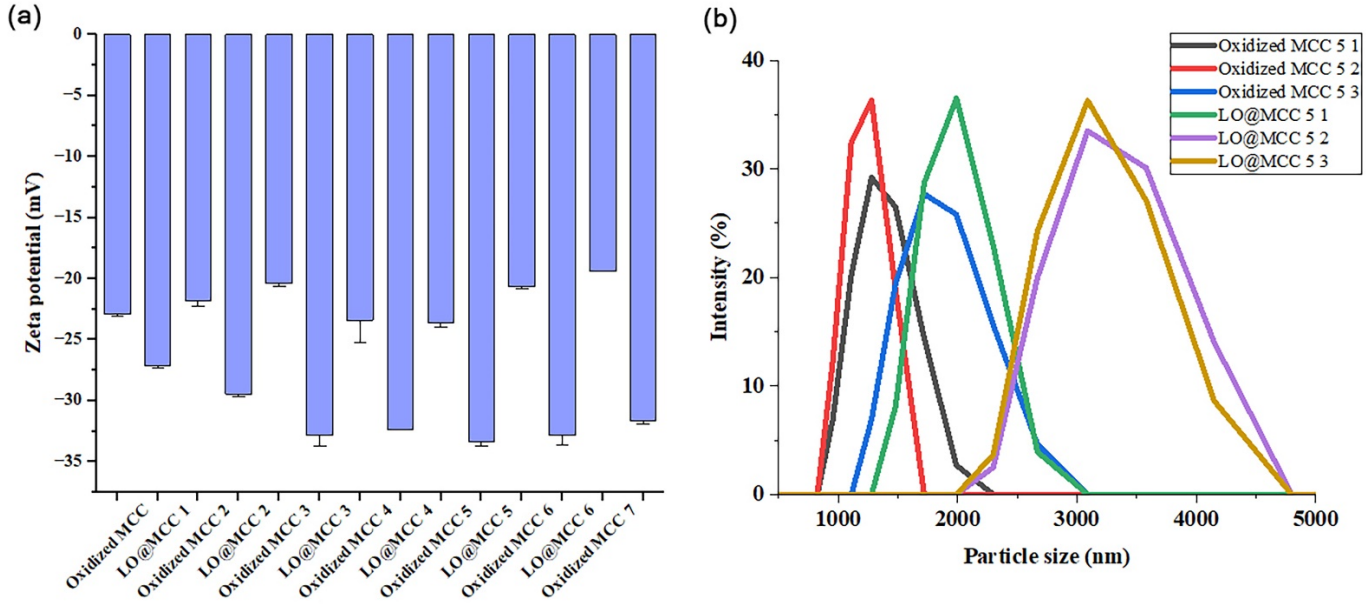

Figure 4 (a) Zeta potential of oxidized MCC and LO@MCC prepared at different EtOH/water ratios: 0/100, 20/80.40/60, 50/50, 60/40, 80/20, and 100/0, and (b) Particle size distribution at EtOH/water ratio of 60/40.

FTIR spectroscopy

FTIR spectroscopy was employed to confirm the success of encapsulation and deposition of LO on the oxidized MCC's surfaces. The spectrum of LO@MCC showed the characteristic bands of LO, confirming the presence of LO on the particle surfaces, as shown in Figure 5.

Morphology of LO@MCC samples

The morphology of LO@MCC 5 samples prepared at an optimum EtOH/water ratio of 60/40 was examined by SEM, compared with oxidized MCC and native MCC, as shown in Figure 6. Native MCC showed fiber morphology with a 20-30 μm diameter. In contrast, oxidized MCC disrupted fiber shape and disintegrated into fragments, with average sizes of around 5-20 μm. This confirms the oxidation and chain scission of the MCC structures. The encapsulated LO@MCC 5 showed a similar shape and morphology to neat oxidized MCC. However, additional white droplets were observed at the particles' surfaces. This is likely LO droplets stabilized by soluble oxidized MCC, forming spherical droplets. The droplets are evidenced as white particles after drying in the SEM sample preparation process. The results confirm that in the oxidation process, MCC molecules were oxidized, converting hydroxyl groups to

carboxylates. Chain scission also occurred, leading to soluble small-sized MCC, while the majority stayed as insoluble fragments with high surface charges, forming stable dispersing particles. In the LO encapsulation process, the soluble MCC acted as a surfactant and shell structure, forming LO-encapsulated droplets, which deposited on the dispersing MCC particles.

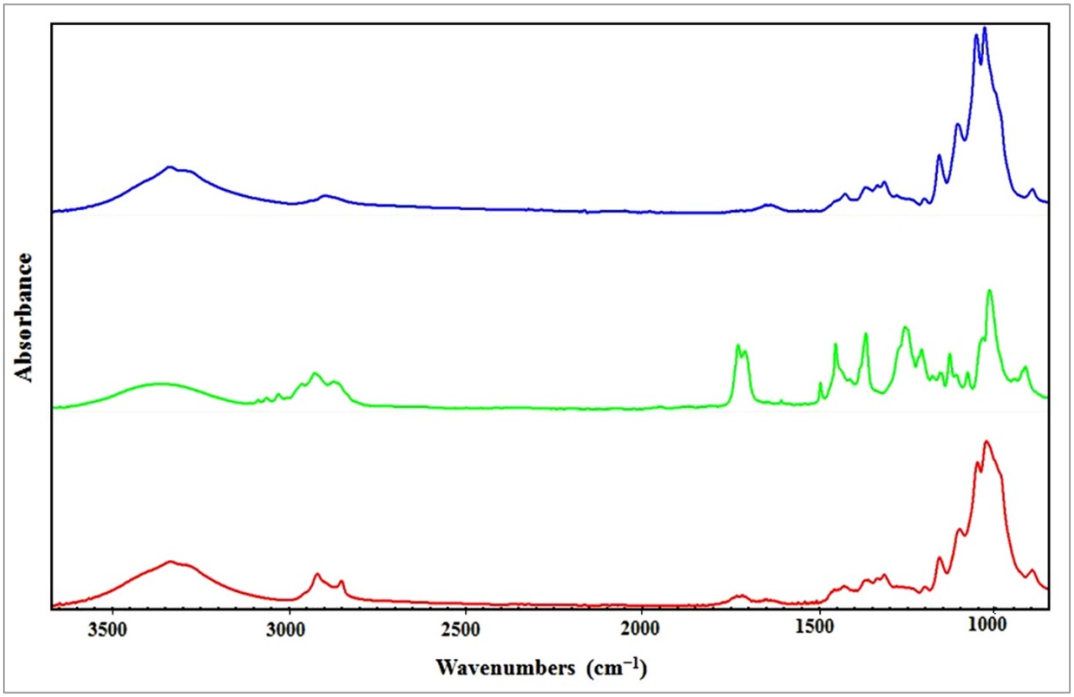

Figure 5 FTIR spectra of LO@MCC 5 (blue), pure LO (green), and oxidized MCC (red).

4. Conclusion

Selective oxidation of MCC using TEMPO and ozone as co-oxidants via a green halogen-free process produced MCC with optimum carboxylic acid/carboxylate contents. The degree of oxidation of hydroxyl to carboxylic acid in MCC depends on reaction time and the acid concentration. The materials were used to encapsulate LO using EtOH/water as a medium, in which an appropriate ratio is 60:40. This mixture enhanced the solubility and dispersion of LO, leading to effective stabilization by MCC and optimized emulsion characteristics. Since MCC was adsorbed around LO to act as a barrier of protection, the size of the encapsulated LO@MCC was greater than the size of the oxidized MCC. The results confirm that in the oxidation process, MCC molecules were oxidized, converting hydroxyl groups to carboxylates. Chain scission also occurred, leading to soluble small-sized MCC, while the majority stayed as insoluble fragments with high surface charges, forming stable dispersing particles. In the LO encapsulation process, the soluble MCC acted as a surfactant and shell structure, forming LO-encapsulated droplets, which deposited on the dispersing MCC particles. The zeta potential of neat oxidized MCC ranges from -20 to -23 mV, reflecting the presence of deprotonated carboxylic acid on its surface. In contrast, LO-encapsulated samples exhibited more negative zeta potential values, ranging from -27 to -33 mV, suggesting an increased deposition of negative charges on the MCC particle surfaces. The higher negative value led to higher particle dispersing stability, preventing agglomeration of the particles. FTIR spectra confirmed the success of LO encapsulation.

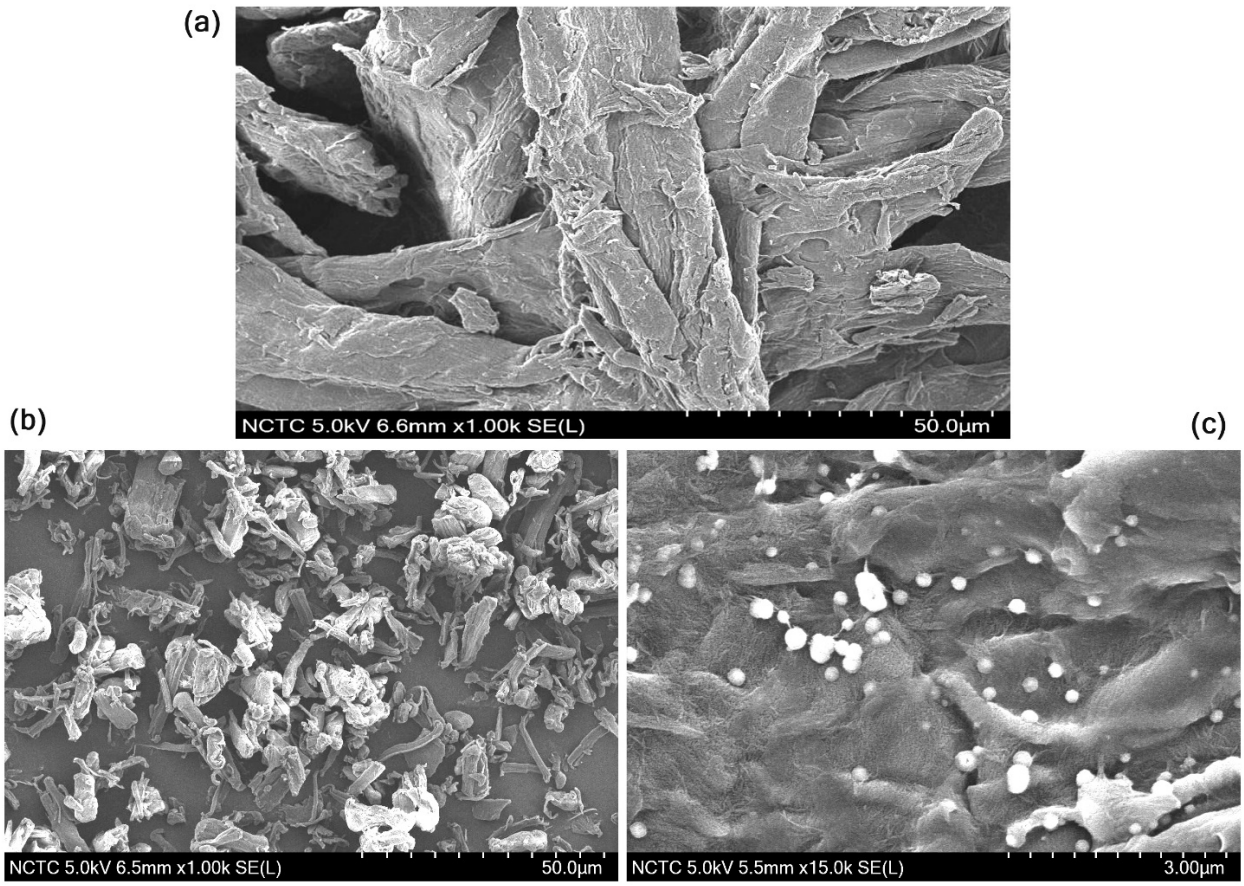

Figure 6 (a) SEM images of native MCC, (b) Oxidized MCC, and (c) LO@MCC prepared at an EtOH/water ratio of 60:40 (LO@MCC 5).

Acknowledgment

Financial support for this work is provided by the Thailand Science Research and Innovation Fundamental Fund and the Center of Excellence in Functional Advanced Materials Engineering (CoE FAME), Thammasat University. G.Y.T.M. acknowledges the scholarship under the Thailand Advanced Institute of Science and Technology and Tokyo Institute of Technology (TAIST-Tokyo Tech) program, awarded by Sirindhorn International Institute of Technology (SIIT), Thammasat University, and the National Science and Technology Development Agency (NSTDA), funded by the National Research Council of Thailand (NRCT).

References

[1] P. Kaewprachu, K. Osako, S. Benjakul, S. Rawdkuen, Effect of protein concentrations on the properties of fish myofibrillar protein-based film compared with PVC film, *J. Food Sci. Technol.* **53** (2016) 2083–2091. [DOI: 10.1007/s13197-016-2170-7].

[2] R. S. Abolore, S. Jaiswal, A. K. Jaiswal, Green and sustainable pretreatment methods for cellulose extraction from lignocellulosic biomass and its applications: A review, *Carbohydr. Polym. Technol. Appl.* **7** (2024) 100396. [DOI:10.1016/j.carpta.2023.100396].

[3] C. Miao, W. Y. Hamad, Cellulose reinforced polymer composites and nanocomposites: A critical review, *Cellulose* **20** (2013) 2221–2262. [DOI: 10.1007/s10570-013-0007-3].

[4] D. Xu, J. Zhang, Y. Cao, J. Wang, J. Xiao, Influence of microcrystalline cellulose on the microrheological property and freeze-thaw stability of soybean protein hydrolysate stabilized curcumin emulsion, *LWT-Food Sci. Technol.* **66** (2016) 590–597. [DOI: 10.1016/j.lwt.2015.11.002].

[5] J. R. T da Silva, E. A de O. Farias, E. C. S. Filho, C. Eiras, Development and characterization of composites based on polyaniline and modified microcrystalline cellulose with anhydride maleic as platforms for electrochemical trials, *Colloid Polym. Sci.* **293** (2014) 1049–1058. [DOI: 10.1007/s00396-014-3489-0].

[6] K. Vanhatalo, T. Lundin, A. Koskimäki, M. Lillandt, O. Dahl, Microcrystalline cellulose property–structure effects in high-pressure fluidization: Microfibril characteristics, *J. Mater. Sci.* **51** (2016) 6019–6034. [DOI: 10.1007/s10853-016-9907-6].

[7] M. Rasheed, M. Jawaid, Z. Karim, L. C. Abdullah, Morphological. physiochemical and thermal properties of microcrystalline cellulose (MCC) extracted from bamboo fiber, *Molecules* **25** (2020) 2824. [DOI:10.3990/molecules 25122824].

[8] C. Yuan, Y. Wang, Y. Liu, B. Cui, Physicochemical characterization and antibacterial activity assessment of lavender essential oil encapsulated in hydroxypropyl-beta-cyclodextrin, *Ind. Crops Prod.* **130** (2019) 104-110. [DOI: 10.1016/ j.indcrop.2018.12.067].

[9] Q. Liu, H. Huang, H. Chen, J. Lin, Q. Wang, Food-grade nanoemulsions: preparation, stability and application in encapsulation of bioactive compounds, *Molecules* **24** (2019) 4242. [DOI: 10.3990/molecules24234242].

[10] A. R. Sheikh, R. A. Wu-Chen, A. Matloob, M. H. Mahmood, M. Javed, Nanoencapsulation of volatile plant essential oils: a paradigm shift in food industry practices, *Food Innov. Adv.* **3** (2024) 305-319. [DOI: 10.48130/fia-0024-0028].

[11] T. P. Le, P. Opaprakasit, Halogen-free "green and mild" process to generate N-oxoammonium cations for use in oxidation of hydroxyls and its quantitative analysis technique and optimization, *Chem. Eng. J.* **429** (2022) 132554. [DOI: 10.1016/j.cej.2021.132554].

[12] S. S. Rahayu, C. Kaewsaneha, P. Opaprakasit, Y. Wongngam, D. Polpanich, Fabrication of lavender essential oil-loaded polyurethane nanoparticles via a facile swelling-diffusion method as hydrocolloid agents for wound healing applications, *Emergent Mater.* **8** (2025) 971–983. [DOI: 10.1007/s42247-024-00887-8].